Percolation with diffusion of particles with attractive interactions

1987 J. Phys. A: Math. Gen. 20 1531

(http://iopscience.iop.org/0305-4470/20/6/035)

J. Phys. A: Math. Gen. **20** (1987) 1531-1542. Printed in UK

Percolation with diffusion of particles with attractive interactions

H O Mártin†‖, E V Albano‡‖ and A L Maltz§

† Laboratorio de Física Teórica, Facultad de Ciencias Exactas, UNLP, CC No 67, (1900) La Plata, Argentina

‡ Instituto de Investigaciones Fisicoquímicas Teóricas y Aplicadas (INIFTA), UNLP, CC No 16, Suc. 4, (1900) La Plata, Argentina

§ Departamento de Matemáticas, Facultad de Ciencias Exactas, UNLP, CC No 172, (1900) La Plata, Argentina

Received 2 April 1986, in final form 4 August 1986

Abstract. The standard percolation model (SPM) is generalised in order to take the diffusion of particles with short-range attractive interaction into account. The movement of particles depends on the temperature and the interaction energy through an external parameter τ ($0 \leqslant \tau \leqslant 1$). Monte Carlo simulations in two dimensions show that the cluster size distribution for small clusters, the number of clusters per site and the percolation threshold substantially change due to the diffusion, depending continuously on τ. The fractal dimension, the correlation length and the percolation probability exponents are calculated. Our study suggests that the proposed model and the SPM belong to the same universality class.

1. Introduction

The standard percolation model (SPM) has been extensively studied in the past due to both the experimental importance of the subject and the interest in the field of phase transitions and critical phenomena, see, for example, the reviews of Stauffer (1979), Essam (1980) and Clerc *et al* (1983). Recently, renewed interest in the SPM has arisen from the study of the fractal properties of clusters at the critical probability. Variants of the SPM consider the case in which the particles, instead of being randomly distributed, are correlated due to interactions between them (Stauffer *et al* 1982 and references therein). The most studied case is the lattice gas (Ising model) where the particles interact via pairwise-additive nearest-neighbour attractive forces (Binder 1979, Stauffer *et al* 1982, Binder 1985). The actual dependence of the interaction energy on the number of neighbours is usually not known and it is expected to be different in specific cases. In fact, based on both experimental results (Fink and Ehrlich 1984) and theoretical studies (Milchev and Binder 1985), it is accepted that, in certain cases, non-pairwise effects are significant. Therefore, we considered it useful to study a percolation model with diffusion (henceforth DPM) where the jumping probability of a given particle depends on whether or not that particle is a monomer. The DPM can be thought of as a Kawasaki dynamics (Kawasaki 1966, Rao *et al* 1976) of a system with *non-additive* lateral interactions.

‖ Financially supported by CONICET, Argentina.

0305-4470/87/061531+12$02.50

Moreover, the DPM allows us to study the structural properties of clusters under thermal equilibrium, which makes a variance with respect to irreversible aggregation of small particles to form fractal structures (Herrmann 1986). In fact, clusters in the DPM can be dissociated in contrast to the kinetic aggregation of particles which is a purely unidirectional process without relation to thermal equilibrium. Only very recently, disaggregation of diffusive particles has been taken into account (Botet and Jullien 1985, Kolb 1986) and the system is studied at its equilibrium regime.

The aim of the present work is to compute directly, by using Monte Carlo simulations, how the diffusion in the steady state regime changes the cluster properties of the DPM close to its percolation threshold compared to those of the static SPM. This is the first time, to our knowledge, that a diffusion model with short-range *non-additive* attractive interactions has been analysed close to its critical percolation region.

The results of Monte Carlo simulations on square lattices are presented and discussed in § 3. In summary the study has been focused on the critical concentration, the correlation length and the percolation probability exponents, the cluster size distribution and the fractal dimension of the largest cluster. Furthermore, in § 3.2 we propose a simple method for comparing the percolation probability exponents of the DPM and SPM when the simulations are carried out using relatively small lattices. Finally, the conclusions are stated in § 4.

2. The model

The crystalline substratum where the diffusion of particles takes place has been represented by a regular bidimensional lattice. Each site of the array can be either occupied by only one particle or empty, i.e. the simulated experiments will be performed within the first monolayer.

Let us now discuss the diffusion of atoms on the lattice. Assuming only attractive nearest-neighbour (NN) site interactions, the 'hopping probability' $\Gamma_{z'}$ for a given particle with z' NN occupied sites is given by Ertl and Küppers (1974) and Bowker and King (1978) (for a review see, for example, King 1980)

$$\Gamma_{z'} = (z - z')\nu_0 \exp[-(E_D + z'w)/kT] \tag{1}$$

where z is the coordination number of the lattice, E_D is the activation energy of diffusion and w is the NN interaction energy. In practice the pre-exponential factor ν_0 is assumed to be a constant (the dependence of ν_0 on the entropy and temperature is neglected or supposed to be dominated by the exponential term of equation (1) (King 1980)).

Based on equation (1) we formulate the rules of the DPM.

(i) Firstly, each site of the lattice is occupied (or empty) with probability $p(1-p$, respectively). This corresponds to the SPM and can be thought of as the condensation of incident atoms onto a cooled substratum.

(ii) After the deposition the motion of the particles starts. At each time step, the probability P_{ij} that a given i particle jumps to one given j NN empty site is

$$P_{ij} = \begin{cases} (zn)^{-1} & \text{if } i \text{ is a monomer.} \\ \tau(zn)^{-1} & \text{if } i \text{ is not a monomer} \end{cases} \tag{2}$$

where a monomer is a particle without NN occupied sites ($z' = 0$), τ ($0 \leqslant \tau \leqslant 1$) is an external fixed parameter throughout all the procedure and n is the total number of

particles on the lattice. Comparing equations (1) and (2), and after an appropriate change of timescale, one has

$$\tau = \exp(-\hat{\omega}/kT) \tag{3}$$

where $\hat{\omega}$ is an effective interaction energy which does not depend on the number of NN occupied sites. That is, the model considers *non-additive* lateral interactions.

Let us note that in the special case $\tau = 1$, where the lateral interaction vanishes, the particles are distributed randomly as in the SPM (Stauffer *et al* 1982). In fact, as will be discussed in § 3, all the results for $\tau = 1$ are in agreement with those obtained with the SPM.

In the present work, Monte Carlo simulations have been performed using the DPM on $L \times L$ square lattices with periodic boundary conditions ($L \leqslant 251$). The initial configuration (IC) is obtained covering the lattice with probability p as in the SPM. Let us denote by an effective movement (EM) when one particle actually jumps from one site to another. When the movement starts, a relaxation period of $2-4n$ EM is generally observed, and then an equilibrium configuration (EC) is obtained. Therefore in order to avoid this 'annealing period', the properties of the layer (such as the distribution of particles in the largest cluster, the cluster size distribution, etc) are calculated for the first time after $12n$ EM. Average values of the properties under investigation are evaluated with subsequent EC, each of them obtained after $2n$ EM. The data for each value of p, L and τ were obtained by averaging over 150-360 EC using 3-30 different IC.

3. Results

3.1. The critical concentration and the correlation length exponent

In the DPM the concentration ϕ is defined as the average number of particles per lattice site. Note that the value of ϕ is equal to the probability p in the starting SPM. Nevertheless, the meaning of ϕ and p is different because, after the diffusion and due to the interactions, the probability of a given site to be occupied is no longer independent of whether other sites are occupied or empty.

Let us denote by ϕ_c (p_c for the SPM) the critical concentration (probability), i.e. for $\phi > \phi_c (p > p_c)$ an infinite cluster appears in the thermodynamic limit; and by $\phi_L (p_L)$ the L-dependent threshold on a lattice of linear size L. In the SPM and for p close to p_c, the correlation length ξ in the infinite system behaves as

$$\xi \sim (p - p_c)^{-\nu} \tag{4}$$

where ν is the correlation length exponent. Thus according to the finite-size scaling (Fisher 1971, Herrmann and Stauffer 1984)

$$p_c = p_L + AL^{-1/\nu}. \tag{5}$$

If, for the DPM, ν^* was the correlation length exponent, then an equivalent expression to equation (5) should be valid, i.e.

$$\phi_c = \phi_L + A^* L^{-1/\nu^*}. \tag{6}$$

Therefore, evaluating ϕ_L for different L, it would be possible to extrapolate the value of ϕ_c using equation (6).

On a $L \times L$ square lattice with periodic boundary conditions a percolating cluster is a cluster which has either its length or its width (or both) equal to L. Let F_L be the fraction of percolating clusters evaluated for a large number of EC at a fixed concentration. Figure 1 shows $F_L^D(L=201)$ for the DPM with $\tau=0.2$ as a function of ϕ and F_L^S $(L=201)$ for the SPM against p. The difference between these two curves suggests that in the $L=\infty$ limit ϕ_c could not be equal to p_c.

One possibility to define ϕ_L and p_L is by demanding that (see also figure 1)

$$F_L^D(\phi_L) = F_L^S(p_L) = 0.9. \tag{7}$$

Therefore, according to equation (5) and as is shown in figure 2, a plot of p_L against $L^{-1/\nu}$ ($\nu=\frac{4}{3}$ in two dimensions) allows us to obtain $p_c = 0.593 \pm 0.006$. This result agrees with the best available values of $p_c = 0.5927 \pm 0.0001$ for a square lattice (see, for example, Gebele 1984, Rapaport 1985, Derrida and Stauffer 1985). The critical concentration evaluated for the DPM with $\tau=1$ is $\phi_c = 0.593 \pm 0.005 = p_c$ as is expected. In figure 2 the results of ϕ_c obtained for $\tau=0.2$ and $\tau=0.05$ have also been plotted against $L^{-1/\nu}$. The values of ϕ_c obtained for different τ have been listed in figure 2. Let us note that great effort has been made in order to obtain very accurate results of the critical probability for the SPM in different lattices. Although our results are less accurate it is beyond any doubt that ϕ_c continuously changes with τ. It should be mentioned that the straight lines obtained for the DPM suggest that (see equation (6))

$$\nu^* = \nu = \tfrac{4}{3}. \tag{8}$$

Consequently, it seems that the diffusion does not change the value of the correlation length exponent as will be discussed later.

The main results of this section can be summarised in equation (8) as well as by the fact that ϕ_c continuously decreases from $\phi_c = p_c = 0.593$ to $\phi_c = 0.565$ when τ decreases from 1 to 0.05, respectively. Although it is very difficult to work with $\tau < 0.05$ due to the large computation time required, we believe that ϕ_c should monotonically decrease in the limit $\tau \to 0$.

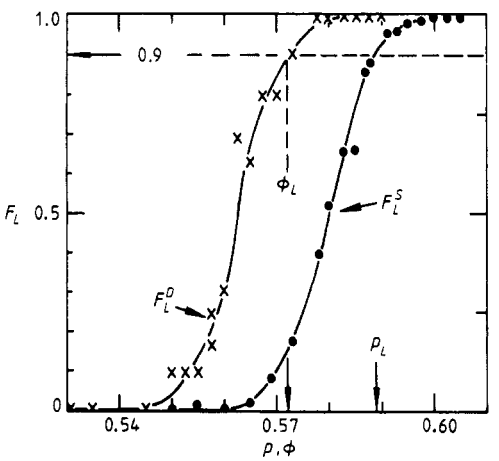

Figure 1. Fraction of percolating clusters F_L^S for the SPM (F_L^D for the DPM) as a function of the probability p (concentration ϕ) on a square lattice of linear size $L=201$. ●, results for the SPM; ×, results for the DPM with $\tau=0.2$. The broken lines show the method employed in the determination of p_L and ϕ_L according to equation (7).

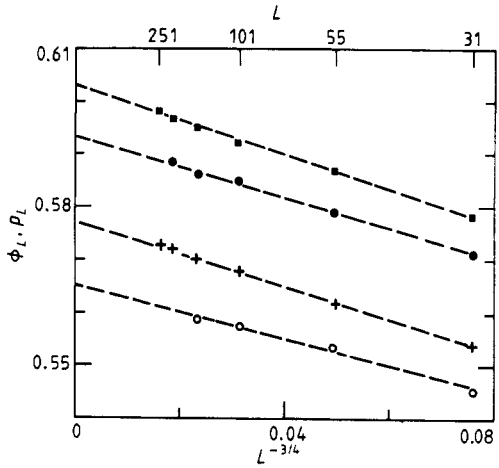

Figure 2. Plot of p_L for the SPM (●, $p_c = 0.593 \pm 0.006$) and ϕ_L for the DPM with different values of τ against $L^{-3/4}$ (see equations (5) and (6)). ■, $\tau = 1.0$ ($\phi_c = 0.593 \pm 0.005$); +, $\tau = 0.2$ ($\phi_c = 0.577 \pm 0.006$); ○, $\tau = 0.05$ ($\phi_c = 0.565 \pm 0.010$). For $\tau = 1$ the ordinate axis has been shifted in 0.1, in order to avoid the superposition with the SPM results. The values of p_c and ϕ_c were obtained by the extrapolation to $L \to \infty$ of the least-squares fit (broken lines). The error bars are large enough in order to take both the error in the determination of each point as well as the possible corrections to equations (5) and (6) due to finite-size effects into account.

3.2. The percolation probability exponent

In our Monte Carlo simulations on square lattices of side L, we define $P_L(\hat{P}_L)$ for the SPM (DPM) by

$$P_L(p) \equiv \frac{S_{max}(p)}{pL^2} \qquad \hat{P}_L(\phi) \equiv \frac{\hat{S}_{max}(\phi)}{\phi L^2} \tag{9}$$

where $S_{max}(\hat{S}_{max})$ is the average number of particles in the largest cluster. In the limit $L \to \infty$, $P_L \to P$ and $\hat{P}_L \to \hat{P}$, these percolation probabilities behave as

$$P \sim (p - p_c)^{\beta} \tag{10a}$$

$$\hat{P} \sim (\phi - \phi_c)^{\beta^*} \tag{10b}$$

for $p(\phi)$ slightly above $p_c(\phi_c)$ (the relation (10a) holds for the SPM and therefore the relation (10b) is expected to be valid for the DPM). Since $\beta = \frac{5}{36}$, β^* can be evaluated from the ratio β/β^*. In fact, let us define $\tilde{p}$ and $\tilde{\phi}$ by demanding that

$$P_L(\tilde{p}) = \hat{P}_L(\tilde{\phi}) \tag{11}$$

then, for large enough L (see equations (10)), one has

$$1 = \frac{\hat{P}_L(\tilde{\phi})}{P_L(\tilde{p})} \sim \frac{(\tilde{\phi} - \phi_c)^{\beta^*}}{(\tilde{p} - p_c)^{\beta}}. \tag{12}$$

In figure 3 a plot of $\ln(\tilde{\phi} - \phi_c)$ against $\ln(\tilde{p} - p_c)$ is shown for the case $\tau = 0.2$. The straight line obtained is in agreement (within an error of 2%) with the equality

$$\beta^* = \beta \tag{13}$$

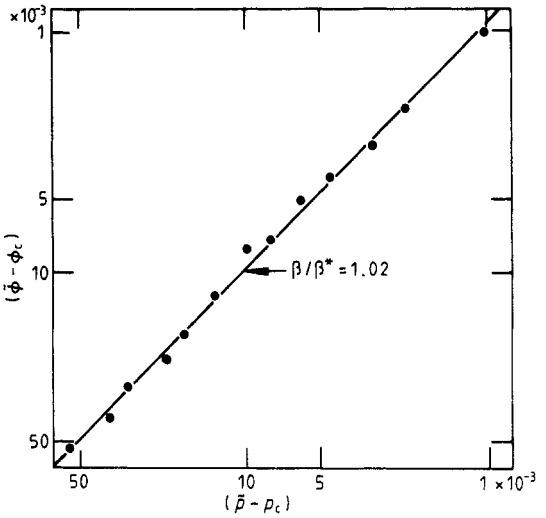

Figure 3. $\ln(\tilde{\phi}-\phi_c)$ plotted against $\ln(\tilde{p}-p_c)$ for $\tau=0.2$ and $L=201$ using $\phi_c=0.577$ and $p_c=0.5927$ (see equation (12)). The full straight line is a least-square fit which gives $\beta/\beta^*=1.02$.

which will be discussed later. Let us stress that, in Monte Carlo simulations, accurate values of β can only be obtained working with very large L. Nevertheless, a good estimation of the ratio β/β^* can be calculated with smaller lattices ($L=201$) as is shown in figure 3.

3.3. The cluster size distribution

Let n_s and $\hat{n}_s$ be the average number of clusters per lattice site containing s sites for the SPM and the DPM respectively. n_s can be calculated exactly for small s, for example on a square lattice one has $n_1=p(1-p)^4$, $n_2=2p^2(1-p)^6$, $n_3=2p^3(1-p)^7(3-p)$, etc. The results of our Monte Carlo simulations agree with these exact cluster numbers within 0.1-0.7% of error. In figure 4(a) the ratio $\hat{n}_s(\phi_c)/n_s(p_c)$ is plotted as a function of s for the case $\tau=0.05$ with $\phi_c=0.565$ and $p_c=0.5927$. Due to the movement with attractive interactions $\hat{n}_s(\phi_c)<n_s(p_c)$ for small s, and as one expects this effect is more important for the monomers. As $p_c>\phi_c$, the number of particles on the lattice is different but our conclusion remains valid since the correction factor to include this effect is $p_c/\phi_c\simeq 1.05$.

Figure 4(b) shows the ratio

$$Y=\sum \hat{n}_s(\phi_c)\left(\sum n_s(p_c)\right)^{-1} \tag{14}$$

for $\tau=0.05$, where the sums run from $s=s_1$ to $s=s_2$ for different values of s_1 and s_2. For the interval between $s_1=1$ and $s_2=100$ we have found that $Y<1$ due to the effect discussed in figure 4(a). For the SPM at the percolation threshold one has the power law behaviour

$$n_s(p_c)\sim s^{-\bar{\tau}} \tag{15}$$

valid for large s, with $\bar{\tau}=187/91\simeq 2.05$ in two dimensions. It should be mentioned that the plot of Y (defined by equation (14)) as a function of s for $s>100$ does not

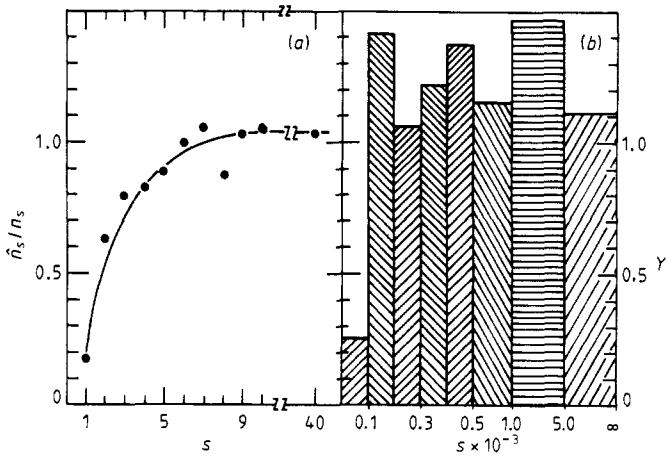

Figure 4. The influence of the diffusion on the cluster size distribution. Comparison between the results for the SPM at $p_c = 0.5927$ and then for DPM at ϕ_c ($\tau = 0.05$) = 0.565 ($L = 201$). (*a*) Plot of the ratio $\hat{n}_s/n_s$ against s for small clusters. (*b*) Plot of Y (see equation (14)) against s for various cluster size intervals. Note that the interval width is not the same in all cases. n_s and $\hat{n}_s$ are obtained by averaging over 250 samples and 195 equilibrium configurations (obtained from 13 different initial configurations), respectively.

show a defined tendency. Then Y could be considered constant within the fluctuations of the simulation. Therefore, this result is in agreement with the behaviour

$$\hat{n}_s(\phi_c) \sim s^{-\bar{\tau}^*} \tag{16}$$

for large enough s with

$$\bar{\tau}^* = \bar{\tau}. \tag{17}$$

A more detailed discussion about the exponents will be presented later.

Figure 5 shows for the DPM (SPM) the average number of clusters per lattice site $\hat{N}_c(N_c)$ as a function of $\phi(p)$ for different values of τ. Taking the definition of $\hat{n}_s$ and n_s into account and for a given value of $\phi = p$, one has

$$\sum s\hat{n}_s = \phi = p = \sum sn_s \tag{18}$$

$$\sum \hat{n}_s = \hat{N}_c \qquad \sum n_s = N_c \tag{19}$$

where the sums run from $s = 1$ to $s = \infty$. It follows from figure 5 that at fixed $\phi = p$ one has $\hat{N}_c \neq N_c$ for $\tau < 1$. Therefore from equations (18) and (19) we conclude that the cluster size distribution must change in the DPM (e.g. for small s, $\hat{n}_s(\phi = p)/n_s(p)$ typically behaves as the curve shown in figure 4(*a*)). Figure 5 also shows that the total number of clusters is reduced when the attractive interaction increases (τ decreases). The values of $\hat{N}_c$ obtained along the broken line $\phi = \phi_c$ do not disagree with figure 4(*b*) and equations (16) and (17) which are only valid for large values of s. In fact, for p close to p_c (in general for p not near 1), the main contribution to N_c (see equation (19)) is due to clusters of small size (say $10 < s$), i.e. just within the interval where the difference between the SPM and the DPM is more important. In other words the change of n_s for small s is relevant in the sense that it makes $\hat{N}_c$ be different from N_c. Results obtained working on smaller lattices with periodic boundary conditions are coincident with those shown in figure 5 for $L = 201$. For example $N_c = 0.0275$ at $p_c = 0.5927$ for

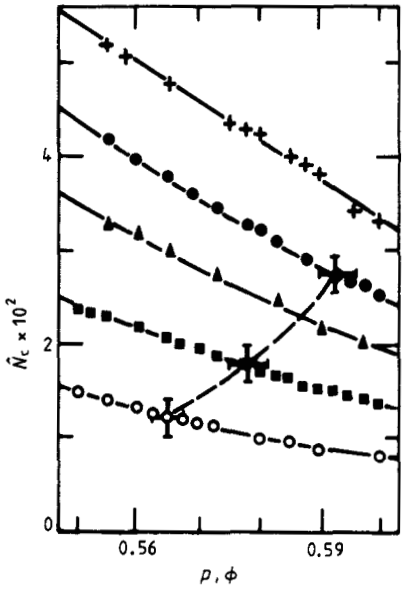

Figure 5. The total number of clusters per lattice site ($L = 201$) $N_c(\hat{N}_c)$ against the probability p (concentration ϕ) for the SPM (●) and for the DPM with different values of τ. +, $\tau = 1$; ▲, $\tau = 0.5$; ■, $\tau = 0.2$; ○, $\tau = 0.05$. For $\tau = 1$ the ordinate axis has been shifted in 0.01. The crosses indicate the position of ϕ_c in the concentration axis and the broken line has been drawn to guide the eyes.

$L = 101$, 151 and 201 and for $\tau = 0.05$ we have obtained $\hat{N}_c = 0.0123$ ($L = 101$), $\hat{N}_c = 0.0122$ ($L = 151$) and $\hat{N}_c = 0.0121$ ($L = 201$) at $\phi_c = 0.565$. Therefore, one should expect that all the results presented in figure 5 would be valid in the thermodynamic limit.

Figure 6 shows the ratio

$$M_1 = \hat{S}_{max}(\phi)/S_{max}(p) \tag{20}$$

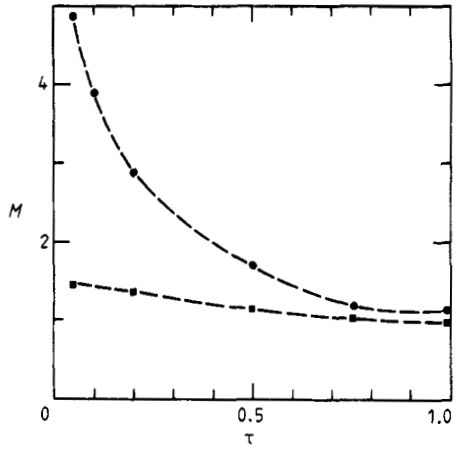

Figure 6. Relative variation of the means cluster size M_1 (●) and M_2 (■), defined by equations (20) and (21) respectively, plotted against τ. $L = 201$ and $\phi = p = 0.565$ which corresponds to the critical concentration for $\tau = 0.05$.

as a function of τ for $p = \phi = 0.565$. One can see from figure 6 how the mass of the largest cluster increases due to the attractive interactions in agreement with the shift of the critical percolation threshold previously discussed. Since $\phi = 0.565$ is our estimated value of ϕ_c for $\tau = 0.05$, an infinite cluster is expected to appear in the thermodynamic limit for $0 \leqslant \tau \leqslant 0.05$, and therefore M_1 should be infinite in this region. The value $M_1 \simeq 5$ obtained for $\tau = 0.05$ is due to the finite-size effect.

From figures 4 and 6 we conclude that the mass of the large cluster increases while the number of small clusters decreases. $\hat{S}_{max}$ increases due to the attachment of individual particles in the boundary of the largest cluster, and also as a consequence of this effect clusters separated by narrow gaps can be joined together. These effects become more important when τ decreases, and this behaviour should also be true in the limit $\tau \to 0$. Nevertheless, the case $\tau = 0$ is worth a further discussion. In fact, at $\tau = 0$ only the monomers can diffuse and stick around the boundary of clusters. Consequently, a 'static' configuration results when monomers are exhausted and the diffusion finishes. On the other hand, we have found that the mass of the largest cluster does not increase as much as for $\tau = 0.05$, and preliminary results indicate that $0.58 \leqslant \phi_c \leqslant 0.59$ which is greater than $\phi_c = 0.565$ for $\tau = 0.05$. Therefore the special case $\tau = 0$ differs from the limit $\tau \to 0$.

Figure 6 also shows the ratio

$$M_2 = \frac{(n - \hat{S}_{max})(\hat{N}_{CL} - 1)^{-1}}{(n - S_{max})(N_{CL} - 1)^{-1}} \tag{21}$$

where $\hat{N}_{CL}(N_{CL})$ is the total number of clusters on the lattice for the DPM (SPM) (remember that n is the total mass on the lattice ($n = \phi L^2 = pL^2$)). That is, the numerator (the denominator) is the average mass per cluster for the DPM (for the SPM respectively) evaluated after the exclusion of the largest cluster. Figure 6 shows that the size of the remaining clusters becomes only slightly enlarged even for the lowest value of τ. This behaviour shows two competitive effects because on one side $\hat{S}_{max}$ increases but on the other the total number of clusters ($N_{CL} = N_c L^2$) decreases (see also figure 5).

Summing up, figures 4–6 show different aspects concerning the modification of the cluster size distribution in the DPM compared with the starting SPM.

3.4. The fractal dimension and the relationship between the exponents

The fractal dimension D of an infinite cluster in d dimensions can be defined by

$$M(l) \sim l^D \tag{22}$$

where M is the number of particles of the cluster within a volume l^d, of linear size l, centred in one point belonging to that cluster. In our two-dimensional simulation we have used squares of side l centred in the geometrical centre of the largest cluster. Figure 7 shows the ln–ln plot of Ml^{-2} as a function of l for both the SPM and the DPM with $\tau = 0.1$, 0.5 and 1.0. In all cases the results presented in figure 7 have been evaluated for concentrations ϕ (probability p) slightly below the critical value $\phi_c(p_c)$. From the slopes of various plots as those shown in figure 7 (for other values of ϕ, τ and L) and using equation (22) we have obtained

$$D = 1.90 \pm 0.02 \tag{23}$$

for $0.1 \leqslant \tau \leqslant 1$ as well as for the SPM.

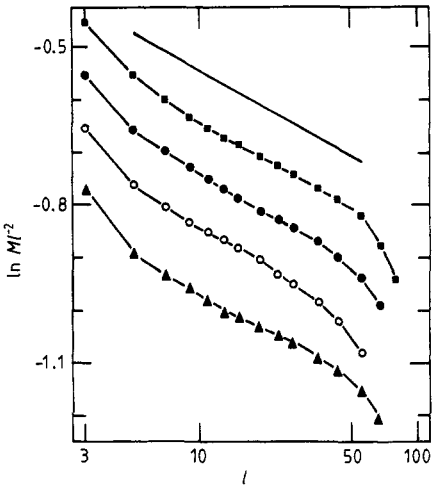

Figure 7. ln-ln plot of Ml^{-2} against l (see equation (22)), with $L = 201$, for both the SPM, ■, $p = 0.583$ averaged over 400 samples; and the DPM for different values of τ. ●, $\tau = 1$, $\phi = 0.583$ (270 EC, 6 IC); ○, $\tau = 0.5$, $\phi = 0.573$ (225 EC, 5 IC); ▲, $\tau = 0.1$, $\phi = 0.560$ (360 EC, 36 IC), n_1EC and n_2IC mean that the value of each point is obtained by averaging n_1 equilibrium configurations using n_2 different initial configurations. For the sake of clarity the results have been shifted on the ordinate axis. The straight full line corresponds to $D = 1.90$.

Let us discuss the relationship between the exponents. Using equations (9) and (10*a*) for the SPM and p close to p_c it follows that

$$M(l, p) \sim (p - p_c)^{\beta} l^{d}. \tag{24}$$

Remembering equation (4) and using the scaling argument for the largest cluster near the critical point, equation (24) also holds replacing ξ by l. Thus from equations (22) and (24) the well known scaling law

$$D = d - \beta/\nu \tag{25}$$

can be obtained (equation (25) is valid for $d \leq d_c$, where $d_c = 6$ is the upper critical dimension). Then, replacing the exact values for two dimensions $\nu = \frac{4}{3}$ and $\beta = \frac{5}{36}$ in equation (25) it follows

$$D = \tfrac{91}{48} \simeq 1.896. \tag{26}$$

Therefore, our result (equation (23)) agrees within the error bars with the expected value of the fractal dimension given by equation (26) (for other Monte Carlo simulations see, for example, Stauffer 1979, 1980, Kapitulnik *et al* 1983).

Using the above arguments, one obviously obtains

$$D = d - \beta^*/\nu^* \tag{27}$$

for the DPM. Comparing equations (23), (25) and (27) it follows that

$$\beta^*/\nu^* = \beta/\nu \tag{28}$$

which are valid within our statistical error. Let us stress that our previous results $\nu^* = \nu$ and $\beta^* = \beta$ (equations (8) and (13)) are in full agreement with the independently obtained equation (28). As in the SPM the standard exponents such as $\alpha, \beta, \gamma, \ldots$, are

related between them (there are only two free exponents), our results (see also equation (17)) strongly suggest that all these exponents take the same values in both models (SPM and DPM) in two dimensions. Other exponents recently introduced and related to the internal structure of the infinite cluster at the critical point as, for example, the fractal dimension of the backbone (Herrmann and Stanley 1984), the spectral dimension and the spreading dimension (see, for example, Vannimenus 1984) have not been evaluated for the DPM. Nevertheless, due to some similarities between the SPM and the DPM as well as for the results previously discussed we would expect that the values of these exponents should be the same for both models.

4. Summary and discussion

A new model of percolation (the SPM defined in § 2), which includes the movement of the particles, is proposed and studied close to the critical concentration. Based on the results discussed in previous sections we state the following conclusions. (i) The critical concentration depends on the interaction between the particles on the lattice. In fact, ϕ_c continuously increases from $\phi_c = 0.565$ for $\tau = 0.05$ up to $\phi_c = p_c = 0.593$ for $\tau = 1$. (ii) The diffusion of particles with attractive interactions simultaneously causes both a strong reduction in the number of small clusters and the growth of large islands. Therefore the cluster size distribution depends on τ. As a consequence of this behaviour the number of clusters per site also changes with τ. (iii) The exponents ν^*, β^* and $\bar{\tau}^*$ and the fractal dimension D do not change with τ ($0.1 \leqslant \tau \leqslant 1$) suggesting that the SPM and the proposed DPM belong to the same universality class (see also the last paragraph of § 3.4). (iv) The DPM is reversible only for $\tau = 1$ where this dynamic model has the same mean values as the SPM for all the analysed magnitudes. In the limit $\tau \to 0$ the DPM is not equivalent to the case $\tau = 0$.

Let us note that for the Ising model it is known that the percolation exponents only change at the thermal critical point (Stauffer *et al* 1982). Our results about universality suggest that, within all the analysed range of τ, the unknown thermal critical point of the DPM has not been reached.

Let us finally discuss some other models related to the percolation theory. The invasion percolation model (with two versions: A without and B with the trapping rule) has been proposed by Wilkinson and Willensen (1983a, b) as a model of fluid displacement in porous media at very low velocity. This model has been extensively studied and, except for the version B in two dimensions, it belongs to the same universality class and has the same values for the percolation threshold as those of the SPM (Wilkinson and Barsony 1984, Mártin *et al* 1984). Nevertheless, the main difference with the SPM arises by the fact that invasion percolation is a dynamic model. In other frameworks, the growth models, such as diffusion-limited aggregation (Witten and Sander 1981) and clustering of clusters (Meakin 1983, Kolb *et al* 1983), have been introduced for the study of the aggregation and the gelation phenomena (for a review see Herrmann 1986). These models have recently been analysed with great interest since the kinetic effects are relevant in the sense that they change the value of the exponents. Nevertheless, these aggregation models are essentially different from the DPM. For example, in the DPM the clusters can be dissociated due to the diffusion of its constituent particles and our study has been performed in the dynamic equilibrium regime, in contrast with the irreversible growth modes where the mass of the largest cluster always increases. On the other hand, reversible aggregation models have recently

been analysed in the steady state equilibrium (Botet and Jullien 1985, Kolb 1986) and the calculated value of the fractal dimension is the same, within the error bars, as that of the static lattice animals but this is not at all a trivial result.

Acknowledgments

One of us (HOM) wishes to express his gratitude to R Gamboa Saraví for stimulating discussions and to J Vannimenus and R Maronna for the information about very good random number generators. We would like to acknowledge the referees for some very useful remarks.

References

Binder K 1979 *Monte Carlo Methods in Statistical Physics* ed K Binder (Berlin: Springer)
—— 1985 *J. Comput. Phys.* **59** 1
Botet R and Jullien R 1985 *Phys. Rev. Lett.* **55** 1943
Bowker M and King D 1978a *Surface Sci.* **71** 583
—— 1978b *Surface Sci.* **72** 208
Clerc J P, Giraud G, Roussenq J, Blanc R, Carton J P, Guyon E, Ottavi H and Stauffer D 1983 *Ann. Phys., Paris* **8** 3
Derrida B and Stauffer D 1985 *J. Physique* **46** 1623
Ertl G and Küppers J 1974 *Low Energy Electrons and Surface Chemistry* ed H F Ebel (Weinhein: Verlag Chemie) p 216
Essam J W 1980 *Rep. Prog. Phys.* **43** 833
Fink H W and Ehrlich G 1984 *Phys. Rev. Lett.* **52** 1532
Fisher M E 1971 *Critical Phenomena. Proc. Enrico Fermi School* vol 51, ed M S Green (New York: Academic) p 1
Gebele T 1984 *J. Phys. A: Math. Gen.* **17** L51
Herrmann H J 1986 *Phys. Rep.* **136** 143
Herrmann H J and Stanley H E 1984 *Phys. Rev. Lett.* **53** 1121
Herrmann H J and Stauffer D 1984 *Phys. Lett.* **100A** 366
Kapitulnik A, Aharony A, Deutscher G and Stauffer D 1983 *J. Phys. A: Math. Gen.* **16** L269
Kawasaki K 1966 *Phys. Rev.* **145** 224
King D 1980 *J. Vac. Sci. Technol.* **17** 241
Kolb M 1986 *J. Phys. A: Math. Gen.* **19** L263
Kolb M, Botet R and Jullien R 1983 *Phys. Rev. Lett.* **51** 1123
Mártin H O, Vannimenus J and Nadal P 1984 *Phys. Rev.* A **30** 3205
Meakin P 1983 *Phys. Rev. Lett.* **51** 1119
Milchev A and Binder K 1985 *Surface Sci.* **164** 1
Rao M, Kalos M H, Lebowtiz J L and Marro J 1976 *Phys. Rev.* B **13** 4328
Rapaport D C 1985 *J. Phys. A: Math. Gen.* **18** L175
Stauffer D 1979 *Phys. Rep.* **54** 1
—— 1980 *Z. Phys.* B **37** 89
Stauffer D, Coniglio A and Adam M 1982 *Adv. Polymer Sci.* **44** 103
Vannimenus J 1984 *J. Physique Lett.* **45** L1071
Witten T A and Sander L M 1981 *Phys. Rev. Lett.* **47** 1400
Wilkinson D and Willensen J F 1983a *Phys. Rev. Lett.* **51** 71
—— 1983b *J. Phys. A: Math. Gen.* **16** 3365
Wilkinson D and Barsony M 1984 *J. Phys. A: Math. Gen.* **17** L129